Diagnostic Study

ANNALS OF MEDICINE & SURGERY

OPEN

Predictive value and potential association of PET/CT radiomics on lymph node metastasis of cervical cancer

Shimin Yang, MD[a], Wenrui Zhang, MD[b], Chunli Liu, MD[b], Chunbo Li, MD, PhD[a,*], Keqin Hua, MD, PhD[a,*]

Objective: Due to the information-rich nature of positron emission tomography/computed tomography (PET/CT) images, the authors hope to explore radiomics features that could distinguish metastatic lymph nodes (LNs) from hypermetabolic benign LNs, in addition to conventional indicators.

Methods: PET/CT images of 106 patients with early-stage cervical cancer from 2019 to 2021 were retrospectively analyzed. The tumor lesions and LN regions of PET/CT images were outlined with SeeIt, and then radiomics features were extracted. The least absolute shrinkage and selection operator (LASSO) was used to select features. The final selected radiomics features of LNs were used as predictors to construct a machine learning model to predict LN metastasis.

Results: The authors determined two morphological coefficient characteristics of cervical lesions (shape – major axis length and shape – mesh volume), one first order characteristics of LNs (first order – 10 percentile) and two gray-level co-occurrence matrix (GLCM) characteristics of LNs (GLCM – id and GLCM – inverse variance) were closely related to LN metastasis. Finally, a neural network was constructed based on the radiomic features of the LNs. The area under the curve of receiver operating characteristic (AUC-ROC) of the model was 0.983 in the training set and 0.860 in the test set.

Conclusion: The authors constructed and demonstrated a neural network based on radiomics features of PET/CT to evaluate the risk of single LN metastasis in early-stage cervical cancer.

Keyword: cervical cancer, lymph node metastasis, PET/CT, radiomics

Introduction

Cervical cancer (CC) is the fourth most common cancer in women, with 604 000 new cases annually worldwide, resulting in 342 000 deaths[1]. The treatment and management of CC is usually guided by the International Federation of Gynecology and Obstetrics (FIGO) staging system, which is based on tumor size, parametrial involvement and pelvic organ invasion without lymph node (LN) involvement. Lymph node metastasis (LNM) has an independent prognostic factor of CC. Therefore, LNM was included for the first time as a key factor in the 2018 update of the FIGO staging system. The updated FIGO staging places greater emphasis on MRI or PET/CT as an accurate measure of LN involvement. If a preoperative examination indicates pelvic LNM, surgery is not necessary and chemoradiotherapy is the first treatment[2,3]. Thus, a preoperative and noninvasive test to determine LN status is significant to select the most appropriate treatment option and avoid unnecessary surgical intervention for CC patients.

Currently, MRI and 2-deoxy-2-fluorodeoxyglucose (^{18}F-FDG) PET/CT have been widely used to assess LN status. Nevertheless, both modalities have their limitations. PET/CT has been shown to be more accurate than MRI in diagnosing LNM[4–6]. However, the ability of PET/CT to discriminate between metastatic LNs and hypermetabolic benign LNs is barely satisfactory[7–9]. In order to improve the accurate of diagnosis, many researchers desire to extract more information from medical images for application in

HIGHLIGHT

- We constructed a neural network based on the radiomics of positron emission tomography/computed tomography to assess the risk of single lymph node metastasis in early-stage cervical cancer. The neural network can stratify patients with high and low risk of lymph node metastasis. Thus, patients can avoid unnecessary treatment and improve their postoperative quality of life.

[a]Department of Gynecology, Obstetrics and Gynecology Hospital of Fudan University and [b]Shanghai Universal Medical Imaging Diagnostic Center, Shanghai, People's Republic of China

Shimin Yang and Wenrui Zhang have contributed equally to this work and share first authorship.

Sponsorships or competing interests that may be relevant to content are disclosed at the end of this article.

*Corresponding author. Address: Department of Gynecology, Obstetrics and Gynecology Hospital of Fudan University, 419 FangXie Road, Shanghai 200011, People's Republic of China. Tel: +863 318 9900, fax: +862 163 455 090. E-mail: huakeqinjiaoshou@163.com (K. Hua), and E-mail: lichunbo142@126.com (C. Li).

Annals of Medicine & Surgery (2024) 86:805–810

Received 18 September 2023; Accepted 9 October 2023

Supplemental Digital Content is available for this article. Direct URL citations are provided in the HTML and PDF versions of this article on the journal's website, www.lww.com/annals-of-medicine-and-surgery.

Published online 7 November 2023

http://dx.doi.org/10.1097/MS9.0000000000001412

oncology. Radiomics is automated high-throughput extraction of quantitative imaging features, followed by the selection of radiomics features related to outcome events to construct a model. Radiomics features are statistical or model-based metrics to quantify tumor intensity, shape, and heterogeneity, which have been shown to reflect intertumoral histopathological properties and to provide prognostic information[10–12]. Compared to commonly used semiquantitative parameters from ^{18}F-FDG PET/CT, such as the standardized uptake value at maximum (SUVmax), recent studies in radiomics have shown the potential added value in the identification and prognostic evaluation of CC[13,14].

Hence, we attempted to discover indicators associated with LNM by PET/CT radiomics and to develop a model to improve the accuracy of the preoperative diagnosis of single LNM.

Methods

Patients

In this retrospective study, we included a total of 106 patients with early-stage CC [IA1 with lymph-vascular space invasion (LVSI), IA2-IIA2].

The inclusion criteria were as follows: (1) patients had no chemotherapy or radiation before PET/CT; (2) the diameter of LN greater than or equal to 2 mm in PET/CT images; (3) pathologic reports indicated the location of metastatic LNs.

The exclusion criteria were as follows: (1) no obvious cervical lesions in PET/CT images; (2) pathologic reports indicated LNM as an isolated tumor cell metastasis; (3) pathologic reports showed that the patient had carcinoma in situ of the cervix.

The patients underwent surgery at the Obstetrics and Gynecology Hospital of Fudan University from 2019 to 2021, who had undergone PET/CT in the 30 days before surgery. All patients performed pelvic LN dissection. However, not all patients performed para-aortic LN dissection. The pathology report at least included metastatic outcomes in the bilateral common iliac LNs and pelvic LNs. All private and image information was kept strictly confidential and only used for the purpose of this research. The ethics committee of the Obstetrics and Gynecology Hospital of Fudan University approved this study.

PET/CT

In this study, we reviewed PET/CT (Biograph-64, Siemens) of CC patients within 30 days before surgery, intercepting images from the first lumbar vertebra to the root of the thigh. Before ^{18}F-FDG injection (2.9–5.6 MBq/kg body weight), the blood glucose level of patients was controlled at less than 10.0 mmol/l. We measured the maximum standardized uptake value of the tumor (tSUVmax), maximum standardized uptake value of the lymph node (nSUVmax), and tumor size in PET/CT. If there was no significant increase in ^{18}F-FDG uptake of the tumor and LNs on PET/CT images, the default SUVmax value was 0. The pathological results served as the gold standard.

Radiomics

The location and metastasis of LNs greater than or equal to 2 mm in diameter and primary cervical lesions in the images were labeled in conjunction with postoperative pathology and SUVmax. According to the description of the number and location of metastatic LNs in the pathology report, metastatic LN regions were localized in PET/CT images. Since previous studies had shown that LNs with a diameter of greater than or equal to 10 mm or high ^{18}F-FDG uptake (especially SUVmax $\geq$ 2.5) had a higher risk of metastasis in PET/CT, metastatic LNs were identified in the localized areas according to the above criteria. Two experienced radiologists will jointly acquire and label the images, but they will independently analyze and interpret LN status in PET/CT before being informed of the pathology results.

In this study, three-dimensional regions (ROIs) of primary CC lesions and labeled LNs based on ^{18}F-FDG PET/CT images were manually outlined and radiomics features were extracted by SeeIt (Version 0.80; https://www.medaifan.net), and radiomics features were extracted. First order features based on histogram analysis were measured by identifying the intensity distribution on the original images, including mean, variability, and skewness. Morphological coefficient features were measured according to the shape, size, and volume of the regions. Higher-order features were measured through parameters such as GLCM, gray-level dependence matrix (GLDM), and gray-level tour matrix (GLRLM). The LASSO analysis further selected radiomics features. Each value contained in each rectangle of the heat map are indicated by a color. In this study, heat maps were used to show the differences between the radiomics features of LNs.

Edge (Version 0.40; https://www.medaifan.net) randomly assigned all LNs to the training sets and test sets in a 7:3 ratio, and built a machine learning model for predicting the risk of LNM based on the radiomics features of LNs. In this study, AUC-ROC was used to assess the diagnostic ability of the model for LNM. We also compared the diagnostic accuracy of independent PET/CT and model for each group of LN status.

The workflow of radiomics was shown in SDC, Figure 1, (Supplemental Digital Content 1, http://links.lww.com/MS9/A302).

Statistical analysis

Edge (Version 0.40; https://www.medaifan.net) were used for statistical analysis. Continuous variables were expressed as mean with SD, and categorical variables were described as frequency with percentage. The correlation between selected radiomic characteristics of cervical lesions and LNs and LNM was investigated through univariate analysis. The results of the univariate analysis to express the strength of the correlation. $P < 0.05$ was statistically significant.

Result

The characteristics of patients were shown in Table 1. A total of 106 patients were included in the study, of whom 54 had negative LNM and 52 had positive LNM. Among patients with negative LNM, 42 (77.8%) patients had a pathologic type of squamous cell carcinoma. The mean (SD) of preoperative SCCA was 2.9 (3.4) ng/ml in patients with negative LNM and 12.5 (16.1) ng/ml in positive LNM patients. Among patients with positive LNM, the mean (SD) of nSUVmax was 7.9 (5.2).

When Lambda was 14.51, the result of LASSO showed that two morphological coefficient features (shape – major axis length and shape – mesh volume) were associated with LNM (Fig. 1). The mean (SD) of shape – major axis length and shape – mesh volume was lower in patients with negative LNM than in patients with positive LNM (Table 1).

Table 1

Characteristics and univariate analysis of the risk of LNM

Variable	Node negative (n=54)	Node positive (n=52)	P
Age (year), n (%)			0.320
< 50	27 (50.0)	21 (40.4)	
≥ 50	27 (50.0)	31 (59.6)	
Menopause, n (%)			0.860
No	30 (55.6)	28 (53.8)	
Yes	24 (44.4)	24 (46.2)	
Number of pregnancies, n (%)			0.532
< 3	24 (44.4)	20 (38.5)	
≥ 3	30 (55.6)	32 (61.5)	
Tumor histology, n (%)			0.808
Squamous cell cancer	42 (77.8)	44 (84.6)	
Adenocarcinoma	7 (13.0)	4 (7.7)	
Adenosequamous cancer	4 (7.3)	3 (5.8)	
Others	1 (1.9)	1 (1.9)	
2018 FIGO stage, n (%)			0.055
IA	2 (3.7)	0 (0.0)	
IB	32 (59.3)	22 (42.3)	
IIA	20 (37.0)	30 (57.7)	
SCCA(ng/ml), mean (SD)	2.9 (3.4)	12.5 (16.1)	< 0.001
Tumor size in PET/CT (cm), mean (SD)	2.7 (1.2)	4.7 (1.4)	< 0.001
tSUVmax, mean (SD)	9.5 (6.3)	13.6 (5.7)	< 0.001
nSUVmax, mean (SD)	0.0 (0.0)	7.9 (5.2)	< 0.001
Radiomic features of cervical lesion			
shape – major axis length, mean (SD)	24.2 (10.0)	43.9 (14.1)	< 0.001
shape – mesh volume, mean (SD)	3491.4 (4353.6)	14168.3 (12311.0)	< 0.001

LNM, lymph node metastasis; nSUVmax, SUVmax of lymph node; PET/CT, positron emission tomography/computed tomography; SCCA, squamous cell carcinoma associated antigen; tSUVmax, SUVmax of tumor.

This study labeled 193 LNs in the PET/CT images. We extracted 107 radiomics features in the outlined LN regions. When the lambda was 11.50, the result of LASSO showed that one first order feature (first order – 10 percentile) and two higher-order features (GLCM – id and GLCM – inverse variance) were associated with LNM (Fig. 2). The heat map showed the differences in the distribution of three radiomics features in the LNs (SDC, Fig. 2, Supplemental Digital Content 2, http://links.lww.com/MS9/A303).

The radiomics features of the LNs were shown in Table 2. The training set contained 135 LNs and the test set included 58 LNs. In both data sets, the mean (SD) of first order – 10 percentile in positive LNM was higher than that in negative LNM, whereas the mean (SD) of GLCM – id and GLCM – inverse variance in positive patients were lower than that in negative patients. First order – 10 percentile, GLCM – id and GLCM – inverse variance were selected as predictors to construct a neural network to assess the risk of single LNM in CC.

The AUC-ROC of the neural network was 0.983 (95% CI: 0.966–1.000) in the training set and 0.860 (95% CI: 0.738–0.982) in the test set, indicating that the neural network had strong discriminative (Fig. 3).

The sensitivity, specificity, positive predictive value, negative predictive value, and accuracy of PET/CT for 193 LNs were 77.0, 83.9, 77.2, 83.7, and 80.3%, respectively. Compared with PET/CT alone, the neural network exhibited higher sensitivity (98.3 and 85.7%) and accuracy (94.8 and 84.5%) in the training set and test set, but slightly lower specificity (75.0%) than PET/CT alone (83.9%) in the test set (Table 3).

Discussion

CC with LNM not only affects prognosis, but also is a pointer to accept radiotherapy. Previous studies have shown that multiple LN metastases increase the risk of recurrence in CC[15,16]. Therefore, clinicians have taken various measures to improve the accuracy of preoperative assessment of LNM, including imaging and LN biopsy[3,17]. The accuracy of diagnostic imaging varies widely across studies, especially as the imaging of benign LNs may appear similar to that of metastatic LNs[18]. Thus, a simple and effective method to predict the risk of LNM can provide

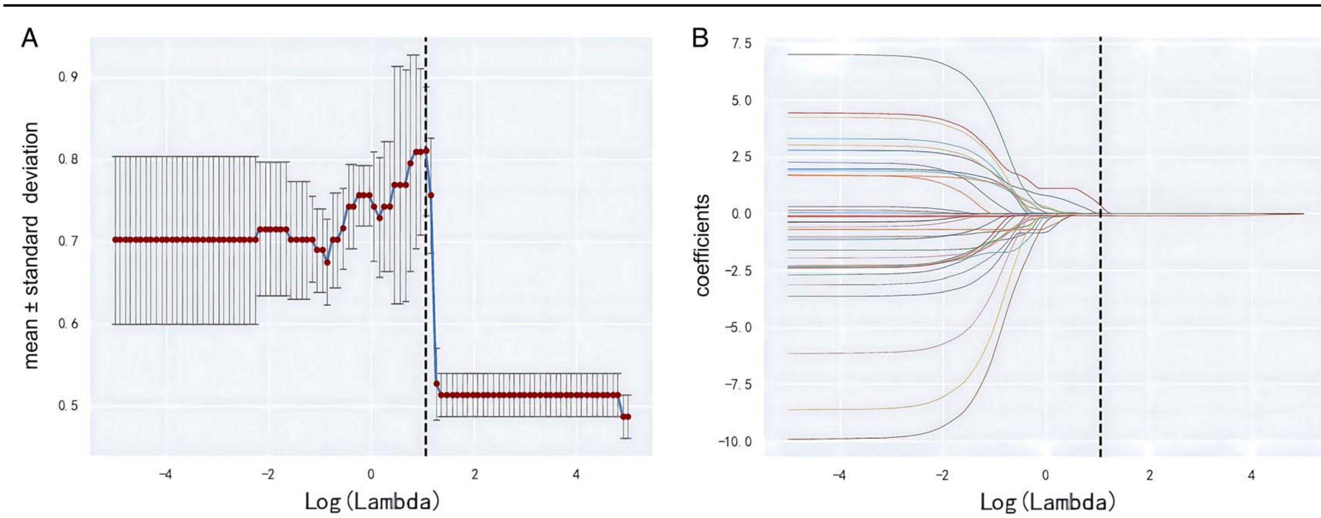

Figure 1. LASSO was used to select radiomics features of primary cervical lesions. When lambda was 14.51, the binomial deviations had the minimum number and two features were selected.

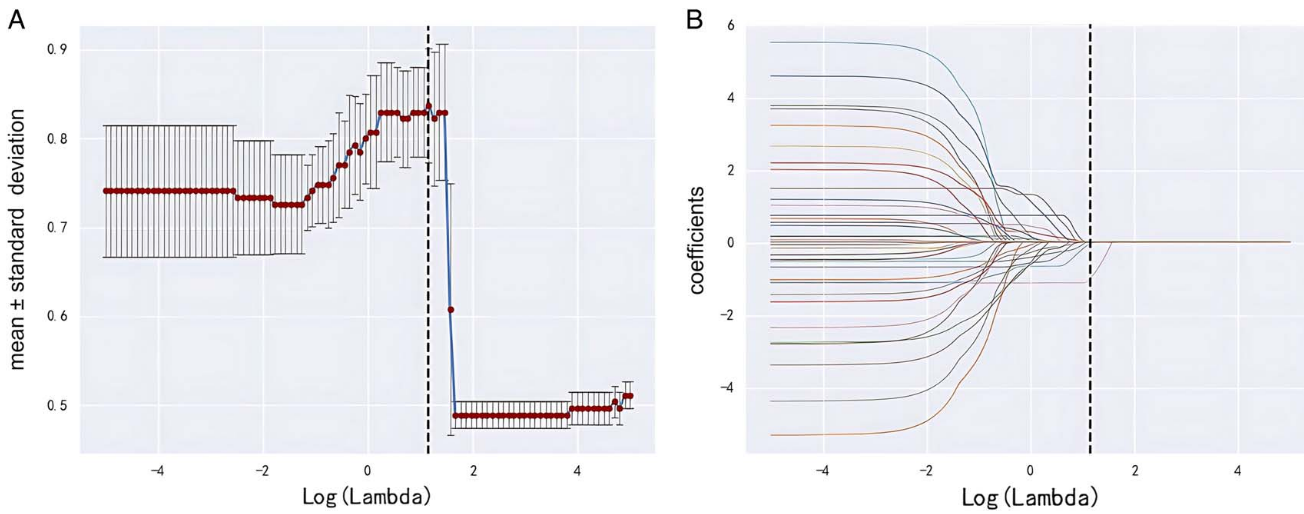

Figure 2. LASSO was used to select radiomics features of lymph nodes. When lambda was 11.50, the binomial deviations had the minimum number and three features were selected.

physicians with important prognostic information and help in the development of treatment. Radiomics, as a new approach, aims to assess tumor heterogeneity by extracting high-throughput features from medical images that reflect underlying pathophysiology[19–21]. In the present study, we constructed and demonstrated a neural network model to evaluate the risk of single LNM in early CC by radiomics.

Recently, radiomics of PET/CT, as an emerging tool, was used for diagnosing tumors, assessing treatment efficacy and predicting prognosis[19,21–23]. The intrinsic biological heterogeneity of malignant tumors leads to changes in radiomics features of the corresponding tumors on PET images. Thus, PET image-based radiomics of primary tumor lesions can reflect the degree of tumor malignancy and correlate with LNM[24–27]. Li *et al.* conducted a retrospective study of 94 patients with early-stage squamous CC. They found that radiomics features of ^{18}F-FDG PET/CT combined with the expression level of vascular endothelial growth factor (VEGF) had significant value in predicting LNM[16]. Similarly, Shen *et al.* confirmed the value of a model-based on the integration of GLCM parameters with SUVmax for the prediction of LNM[28]. The radiomics features in both studies are high-order texture features. In addition to the higher-order texture features, the predictors of our neural network include the first order features.

In our study, shape – major axis length and shape – mesh volume were used as morphological features of primary cervical lesions associated with LNM. Shape-based features describe the geometry of ROIs, which help predict tumor malignancy and treatment response. These features are extracted from the 3D structure of ROIs to measure the shape and size of tumors. It is evident that larger and irregular tumor lesions have a higher risk of LNM. The study also proved that the neural network established by first order – 10 percentile and GLCM parameters (GLCM – id and GLCM – inverse variance) of LN could improve the accuracy of predicting LNM. First order features are based on intensity. The intensity-based approach converts 3D ROIs into individual histograms (describe the distribution of pixel intensity), from which simple features are derived. High-order texture features capture the spatial relationships between adjacent pixels, which have an important part in the studies of tissue heterogeneity. GLCM simulates the spatial distribution of pixel intensity, and from whom the features extracted are the most commonly used texture features[29,30]. The neural networks based on radiomics features of LNs can predict the risk of individual LNM and localize metastatic LNs. If the neural network diagnoses single or multiple LN metastases on PET/CT images, it can guide clinicians to choose radical radiotherapy as the preferred treatment option. It can also develop a radiotherapy plan based on the number and location of metastatic LNs.

Radiomics is a promising approach, but it has some drawbacks. First, the reproducibility of radiomics features varies widely. Most radiomics features are influenced by multiple

Table 2

Radiomics features of lymph nodes and univariate analysis

	Train set			Test set		
	Negative	Positive		Negative	Positive	
Variable	(n=77)	(n=58)	P	(n=16)	(n=42)	P
first order – 10 percentile, mean (SD)	134.8 (134.9)	472.9 (290.6)	< 0.001	224.8 (146.9)	472.2 (271.8)	< 0.001
GLCM – id, mean (SD)	0.7 (0.2)	0.3 (0.2)	< 0.001	0.5 (0.2)	0.3 (0.1)	< 0.001
GLCM – inverse variance, mean (SD)	0.5 (0.2)	0.2 (0.2)	< 0.001	0.4 (0.2)	0.2 (0.1)	< 0.001

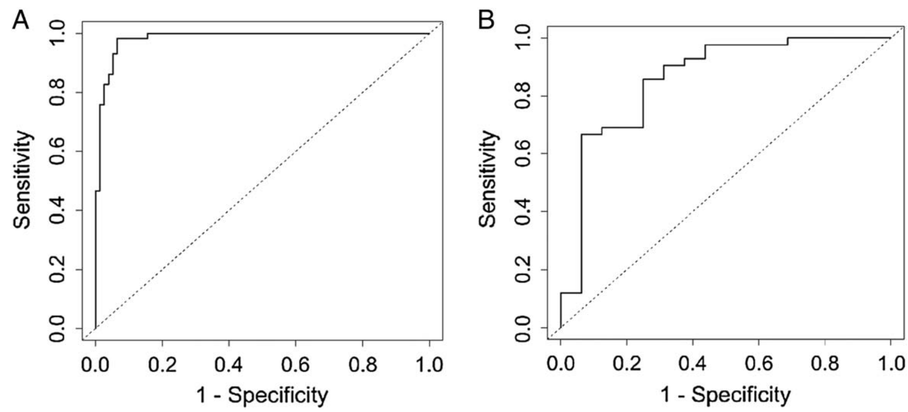

Figure 3. The AUC-ROC of the neural network in the training set (A) and test set (B).

factors, such as scanners, reconstruction algorithms, tumor segmentation methods, and quantization processes[4,31,32]. The standardization of image acquisition and feature extraction is one of the prerequisites for the application of radiomics in clinical practice. The accurate delineation of the lesion is an important step in the extraction of radiological features as the features come from the delineated region[10,33]. In our study, we chose to delineate the target area manually. Secondly, the naming, definition, and analysis methods of radiomics features are not consistent in various clinical studies, which makes it difficult to compare the results of various studies[34–36]. Meanwhile, some researchers emphasize that most published radiomics models have never been validated in an external multicenter setting. Addressing these issues is crucial for the future successful application of radiomics in clinical practice.

Similarly, our study has some limitations. First, as a single-center retrospective study, we need a multicenter large-sample prospective study to further confirm the findings. Second, the collected pathologic data did not accurately report the anatomical relationship of metastatic LNs to the surrounding vascular tissue, which may lead to errors when labeling LN status on PET/CT images. Finally, the predominant tissue type of CC was squamous cell carcinoma in our research. Adenocarcinoma, adenosquamous carcinoma and rare types of CC require further study.

Despite these limitations, we were the first study to construct a neural network to predict the risk of single LNM in early-stage CC based on the radiomics features of LNs. Both the training and test set showed potential associations between LNM and radiomics features in CC. Finally, it was found that first order – 10 percentile, GLCM – id and GLCM – inverse variance in ^{18}F-FDG PET/CT were predictors of LNM. These radiomics features of PET/CT are available in daily practice and more valuable than independent PET/CT, which is another advantage. After identifying patients at high risk with LNM through the model, clinicians can individualize treatment, including increasing the dose of radiotherapy and expanding the scope of radiotherapy.

Table 3

Accuracy values of PET/CT and neural network in LNM

Variable	PET/CT	Neural network Train set	Neural network Test set
Sensitivity (%)	77.0	98.3	85.7
Specificity (%)	83.9	93.5	75.0
Negative predictive value (%)	77.2	98.6	66.7
Positive predictive value (%)	83.7	91.9	90.0
Accuracy (%)	80.3	94.8	84.5

Conclusion

Above all, we demonstrated that radiomics features of PET/CT had the potential to predict LNM and could be used as a predictor of LNM. Meanwhile, the neural network model can stratify patients with high and low risk of LNM to avoid unnecessary treatment and improve postoperative quality of life.

Ethical approval

The ethics committee of Obstetrics and Gynecology Hospital of Fudan University approved this study (No.2020-183).

Consent

Written informed consent was obtained from the individual(s) for the publication of any potentially identifiable images or data included in this article. A copy of the written consent is available for review by the Editor-in-Chief of this journal on request.

Sources of funding

This study was supported by the Clinical Research Plan of SHDC (SHDC2020CR1045B, SHDC2020CR6009) to KQ Hua, the Shanghai Municipal Health Commission (20194Y0085) to CB Li, and the Shanghai ‘Rising Stars of Medical Talent’ Youth Development Program (SHWSRS2020087) to CB Li.

Author contribution

S.Y. and W.R.Z.: contributed equally to this work; S.M.Y., W.R.Z., and C.L.L.: collected the data and did the statistical analysis; S.M.Y.: organized and submitted the manuscript; K.Q.H. and C.B.L.: guided the whole process.

Conflicts of interest disclosure

The authors declare there was no commercial or financial conflicts of interest.

Research registration unique identifying number (UIN)

Our study is a retrospective analytical study. Therefore, we did not register.

Guarantor

Shimin Yang, Wenrui Zhang, Chunli Liu, Chunbo Li, and Keqin Hua.

Data availability statement

The original contributions presented in the study are included in the article/supplementary material. Further inquiries can be directed to the corresponding authors.

Provenance and peer review

Our paper was not invited.

References

[1] Sung H, Ferlay J, Siegel R, *et al*. Global cancer statistics 2020: GLOBOCAN estimates of incidence and mortality worldwide for 36 cancers in 185 countries. CA Cancer J Clin 2021;71:209–49.

[2] Wu Q, Wang S, Zhang S, *et al*. Development of a deep learning model to identify lymph node metastasis on magnetic resonance imaging in patients with cervical cancer. JAMA Network Open 2020;3:e2011625.

[3] Lee SI, Atri M. 2018 FIGO staging system for uterine cervical cancer: enter cross-sectional imaging. Radiology 2019;292:15–24.

[4] Ai Y, Zhu H, Xie C, *et al*. Radiomics in cervical cancer: current applications and future potential. Crit Rev Oncol Hematol 2020;152:102985.

[5] Yang S, Liu C, Li C, *et al*. Nomogram predicting lymph node metastasis in the early-stage cervical cancer. Front Med 2022;9:866283.

[6] Liu S, Feng Z, Zhang J, *et al*. A novel 2-deoxy-2-fluorodeoxyglucose ((18) F-FDG) positron emission tomography/computed tomography (PET/CT)-based nomogram to predict lymph node metastasis in early stage uterine cervical squamous cell cancer. Quant Imaging Med Surg 2021;11:240–8.

[7] Nguyen N, Beriwal S, Moon C, *et al*. Diagnostic value of FDG PET/MRI in females with pelvic malignancy-a systematic review of the literature. Front Oncol 2020;10:519440.

[8] Zheng M, Xie D, Pan C, *et al*. Diagnostic value of 18F-FDG PET/MRI in recurrent pelvis malignancies of female patients: a systematic review and meta-analysis. Nucl Med Commun 2018;39:479–85.

[9] Anner P, Mayerhöfer M, Wadsak W, *et al*. [F]FDG-PET/CT and MRI for initial pelvic lymph node staging in patients with cervical carcinoma: the potential usefulness of FDG-PET/MRI. Oncol Lett 2018;15:3951–6.

[10] Lucia F, Visvikis D, Desseroit M, *et al*. Prediction of outcome using pretreatment F-FDG PET/CT and MRI radiomics in locally advanced cervical cancer treated with chemoradiotherapy. Eur J Nucl Med Mol Imaging 2018;45:768–86.

[11] Ho K, Fang Y, Chung H, *et al*. A preliminary investigation into textural features of intratumoral metabolic heterogeneity in (18)F-FDG PET for overall survival prognosis in patients with bulky cervical cancer treated with definitive concurrent chemoradiotherapy. Am J Nucl Med Mol Imaging 2016;6:166–75.

[12] Reuzé S, Orlhac F, Chargari C, *et al*. Prediction of cervical cancer recurrence using textural features extracted from 18F-FDG PET images acquired with different scanners. Oncotarget 2017;8:43169–79.

[13] Mu W, Liang Y, Hall L, *et al*. F-FDG PET/CT habitat radiomics predicts outcome of patients with cervical cancer treated with chemoradiotherapy. Radiol Artif intell 2020;2:e190218.

[14] Ferreira M, Lovinfosse P, Hermesse J, *et al*. [F]FDG PET radiomics to predict disease-free survival in cervical cancer: a multi-scanner/center study with external validation. Eur J Nucl Med Mol Imaging 2021;48:3432–43.

[15] Bhatla N, Berek J, Cuello Fredes M, *et al*. Revised FIGO staging for carcinoma of the cervix uteri. Int J Gynaecol Obstet 2019;145:129–35.

[16] Li K, Sun H, Lu Z, *et al*. Value of [F]FDG PET radiomic features and VEGF expression in predicting pelvic lymphatic metastasis and their potential relationship in early-stage cervical squamous cell carcinoma. Eur J Radiol 2018;106:160–6.

[17] Liu J, Liu X, Guo Z, *et al*. Ultrasound-guided fine needle aspiration cytology of Para-aortic lymph node metastasis in uterine cervical cancer: diagnostic accuracy and impact on clinical decision making. BMC Cancer 2021;21:964.

[18] Wu Q, Wang S, Chen X, *et al*. Radiomics analysis of magnetic resonance imaging improves diagnostic performance of lymph node metastasis in patients with cervical cancer. Radiother Oncol 2019;138:141–8.

[19] Bizzarri N, Russo L, Dolciami M, *et al*. Radiomics systematic review in cervical cancer: gynecological oncologists' perspective. Int J Gynecol Cancer 2023;33:1522–41.

[20] Manganaro L, Nicolino G, Dolciami M, *et al*. Radiomics in cervical and endometrial cancer. Br J Radiol 2021;94:20201314.

[21] Liu Z, Wang S, Dong D, *et al*. The applications of radiomics in precision diagnosis and treatment of oncology: opportunities and challenges. Theranostics 2019;9:1303–22.

[22] Sun C, Tian X, Liu Z, *et al*. Radiomic analysis for pretreatment prediction of response to neoadjuvant chemotherapy in locally advanced cervical cancer: a multicentre study. EBioMedicine 2019;46:160–9.

[23] Autorino R, Gui B, Panza G, *et al*. Radiomics-based prediction of two-year clinical outcome in locally advanced cervical cancer patients undergoing neoadjuvant chemoradiotherapy. Radiol Med (Torino) 2022;127:498–506.

[24] Li X, Xu C, Yu Y, *et al*. Prediction of lymphovascular space invasion using a combination of tenascin-C, cox-2, and PET/CT radiomics in patients with early-stage cervical squamous cell carcinoma. BMC Cancer 2021;21:866.

[25] Antunovic L, De Sanctis R, Cozzi L, *et al*. PET/CT radiomics in breast cancer: promising tool for prediction of pathological response to neoadjuvant chemotherapy. Eur J Nucl Med Mol Imaging 2019;46:1468–77.

[26] Liu Z, Li Z, Qu J, *et al*. Radiomics of multiparametric MRI for pretreatment prediction of pathologic complete response to neoadjuvant chemotherapy in breast cancer: a multicenter study. Clin Cancer Res 2019;25:3538–47.

[27] Tian Y, Liu Z, Tang Z, *et al*. Radiomics analysis of DTI data to assess vision outcome after intravenous methylprednisolone therapy in neuromyelitis optic neuritis. J Magnetic Resonance Imag 2019;49:1365–73.

[28] Shen W, Chen S, Liang J, *et al*.[18] Fluorodeoxyglucose positron emission tomography for the textural features of cervical cancer associated with lymph node metastasis and histological type. Eur J Nucl Med Mol Imaging 2017;44:1721–31.

[29] Afshar P, Mohammadi A, Plataniotis KN, *et al*. From handcrafted to deep-learning-based cancer radiomics: challenges and opportunities. IEEE Signal Process Magaz 2019;36:132–60.

[30] Shakir H, Khan T, Rasheed H, *et al*. Radiomics based bayesian inversion method for prediction of cancer and pathological stage. IEEE J Transl Eng Health Med 2021;9:4300208.

[31] Limkin E, Sun R, Dercle L, *et al*. Promises and challenges for the implementation of computational medical imaging (radiomics) in oncology. Ann Oncol 2017;28:1191–206.

[32] Dercle L, Henry T, Carré A, *et al*. Reinventing radiation therapy with machine learning and imaging bio-markers (radiomics): State-of-the-art, challenges and perspectives. Methods (San Diego, Calif) 2021;188:44–60.

[33] Eminowicz G, McCormack M. Variability of clinical target volume delineation for definitive radiotherapy in cervix cancer. Radiother Oncol 2015;117:542–7.

[34] Lucia F, Visvikis D, Vallières M, *et al*. External validation of a combined PET and MRI radiomics model for prediction of recurrence in cervical cancer patients treated with chemoradiotherapy. Eur J Nucl Med Mol Imaging 2019;46:864–77.

[35] Zwanenburg A, Lock S. Why validation of prognostic models matters? Radiother Oncol 2018;127:370–3.

[36] Vallières M, Zwanenburg A, Badic B, *et al*. Responsible Radiomics Research for Faster Clinical Translation. J Nucl Med 2018;59:189–93.